An Investigation of Parametric Load Leveling Control Methodologies for Resistive Heaters in Smart Grids

Lee Holland, *Student Member, IEEE,* H. Bora Karayaka, *Senior Member, IEEE,* Martin L. Tanaka and Aaron Ball
Department of Engineering and Technology
Western Carolina University
Cullowhee, North Carolina USA
hbkarayaka@wcu.edu

***Abstract*— The main goal in this study is to demonstrate that load leveling with demand side management in smart grids can be achieved to reduce peak power consumption while maintaining residential room temperatures at a comfortable level. A prototype enclosure was built and equipped with a heater and thermal measuring equipment. Data was collected during a 17 hour temperature regulation experiment using a traditional on-off (bang-bang) controller similar to those commonly used for residential heating control. A second order mathematical model was utilized to estimate the net thermal resistances and capacitances using system identification techniques at two different temperature set points. The enclosure system was used to determine if peak power could be reduced by slowly varying loads utilizing a different type of controller. Two different linear control techniques (using K-Factor and PI approaches) and the associated power electronics circuitry were implemented and tuned. Both controller systems successfully leveled the load and reduced the peak power demand.**

***Index Terms*—System Identification, Load Leveling, Linear Control, Smart Grids.**

I. INTRODUCTION

One large target for load leveling is space heating appliances and other Thermostatically Controlled Appliances (TCA's). In 2004, residential buildings accounted for over 20% of the primary energy consumption in the U.S. [1]. Also, the US, single family residential houses consume up to 66% of their energy from controllable appliances, with 41% from space heaters alone [2]. Controllable appliances also include electric water heaters, ovens, air conditioners, refrigerators, and dishwashers.

Demand Side Management (DSM) is a powerful tool to provide fast response ancillary service for utilities [3]. For this reason, utilities try to reflect the cost of generating electricity in customer pricing schedules (Table 1). In this context, Direct Load Control (DLC) and Indirect Load Control (ILC) also offer ways to shift peak loads to non-peak times. Load shifting does not reduce total energy consumed but shifts loads when demand for energy is large to when demand is smaller. DLC offers direct control for utility companies, and can offer large ancillary service with aggregated use. With IDC, appliances can independently operate when desired, in response to dynamic pricing or temperature levels in the case of TCA's [4,5]. An example of dynamic pricing strategies can be seen in Table 1.

TABLE 1 – North America Proposed Pricing Structures [6]

	Pricing Strategies in North America		
Structure	***Time of Day***	***Cost (Cents/kWh)***	***Additional Information***
Flat Rate		6	First 600kWh of Summer
(FR)		7	Additional Use
Time of Use	10pm-7am	4	off-peak
(TOU)	7am-11am	8	mid-peak
	11am-5pm	11	On-peak
Critical Peak Pricing	10pm-7am	3	off-peak
(CPP)	7am-11am 5pm-10pm	8	mid-peak
	11am-5pm	11	On-peak
	Event block	30	CPP 3-4 Hour Event Block
Real Time Pricing	Average	5	Price Changes relative to actual Power Generation
(RTP)	Maximum	35	

This paper proposes a novel IDC scheme that can significantly level the power used for space heating. Typically space heaters are controlled in a bang-bang manner which can cause large spikes of power. When a TCA has a small duty cycle, there may be large variations in thermal comfort and power used. With a slowly varying load, the heating is much more consistent and can also reduce the large instantaneous demands of power from space heaters.

This project is supported in part by the Center for Rapid Product Realization at Western Carolina University.

In this paper two linear control schemes using standard PI and K-Factor approach [7] are designed and simulated. The latter will be referenced as Phase Boost controller throughout the paper. Lumped capacitance model thermal systems from the experimental system identification study are utilized in designing these controllers. System identification was performed for a 32° C and 25° C test with 20° C ambient temperatures. The controllers' performance was extensively tested and compared to a traditional bang-bang controller.

II. Thermal System Modeling and Simulation

A. Lumped Capacitance Circuit Model

In order to control a thermal system through simulations, a transfer function for the system model is needed. A low order electrical circuit representation of a system can be developed using the physical characteristics of a building. In practice modeling is done with lumped parameters using resistors for insulation and capacitors for thermal masses. The mass flow into a thermal system is represented by the current into the circuit, and the voltage at a node represents the temperature in degrees Celsius at that node. [8]

In the first phase of this study an enclosure model was identified using a second order thermal system in Matlab [9]. In this system, V_{room}, V_{heater}, and $V_{ambient}$ are the temperatures of the room, heater, and outside environment, respectively. P_{in} is the input power for the system. A state space representation is used where x_1 is equal to V_{heater}, x_2 is equal to V_{room} and the output, y, is equal to x_2. R_1, R_2 and R_3 are the thermal resistances for heater, air and enclosure, respectively. The capacitor (C_1) and (C_2) are used to model combined heater and air thermal capacitances in the room. Equation 1 gives the state space form for the system modeled.

$$\begin{pmatrix}\dot{x}_1\\ \dot{x}_2\end{pmatrix} = \begin{pmatrix}\frac{-1}{R_2C_1} & \frac{1}{R_2C_1}\\ \frac{1}{R_2C_2} & \frac{-1}{R_2C_2}-\frac{1}{R_3C_2}\end{pmatrix}\begin{pmatrix}x_1\\ x_2\end{pmatrix} + \begin{pmatrix}0\\ \frac{1}{R_3C_2}\end{pmatrix}V_1 + \begin{pmatrix}\frac{1}{C_1}\\ 0\end{pmatrix}P_{in}$$

$$y = x_2 \qquad (1)$$

The system was later modeled in PSpice [10] as seen in Figure 1. The ambient temperature was modeled with a DC source for the constant ambient temperature, and a DC biased AC source for the variable ambient temperature. A voltage dependent current source with two multiplied inputs (G9) was used to generate the electrical power for the thermal system. The initial condition of the capacitors was set to the starting ambient temperature in the enclosure. In Figure 1, model parameters R_1, R_2, R_3, C_1 and C_2 are represented by R_{17}, R_{14}, R_{13}, C_9 and C_8 respectively.

B. System Identification Results

A prototype enclosure was built and equipped with a heater and thermal/electrical measuring equipment. This enclosure was later heated to 25° C and 32° C with a traditional bang-bang controller. Data was collected during a 17 hour temperature regulation experiment. Adaptive Gauss Newton "gna" least squares optimization algorithm was employed in the identification process [9] to obtain the operating point dependent thermal model parameters (Table 2). The resistance R_1 is not identifiable based on the model equation (1) unless additional heater core temperature measurements are conducted (which is the beyond the scope of this study).

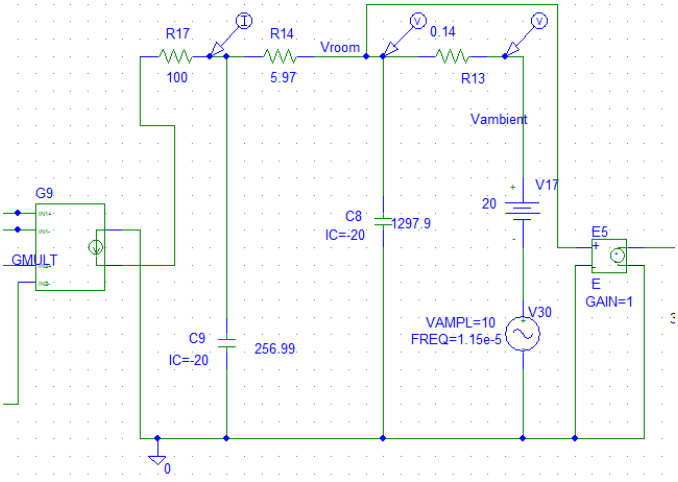

Figure 1– Two Capacitance Thermal Model Stage in PSpice

TABLE 2 – Identified Thermal Enclosure System Parameters with Electrical Equivalents

	System Identification Results				
Model	**Set-point**	**R_2 (Ω)**	**R_3 (Ω)**	**C_1 (F)**	**C_2 (F)**
1	25 C	6.55	0.08	120.67	3135.00
2	32 C	5.97	0.14	256.99	1279.90

III. Control Methodology

A general control scheme was designed in the implementation of each controller. Steady state error is the set-point temperature, T_{sp}, minus the room temperature, T_{room}. The steady state error was used as feedback in the closed loop system (Figure 2). In order to design the controller, a transfer function is needed for each of the other system blocks. From the system identification study a thermal transfer function was found for both the 25° C and 32° C set-points. An example thermal system transfer function (with power input and room temperature output) can be seen in equation 2, where the state space model of the 32 degree system identification was converted to a transfer function using appropriate Matlab functions. The controller transfer function is different for each design and will be introduced accordingly.

$$G_T(s) = \frac{5\cdot 10^{-7}}{s^2 + 0.006s + 3.6\cdot 10^{-6}} \qquad (2)$$

A DC-DC buck converter power stage due to its near linear characteristics was selected. In order to match the power stage to the real system, a 120V DC input (120 V_{rms} AC equivalent) was assumed, with an 87.53Ω load resistor. For this controller Continuous Conduction Mode (CCM) was desired. Operation in Discontinuous Conduction Mode (DCM) is allowed in this design, and utilized solely for the bang-bang controller. The linearized transfer function for the buck converter $G_{PS}(s)$in this system can be seen in equation 3 [11].

$$G_{PS}(s) = \frac{V_{in}}{LC}\frac{1+srC}{s^2 + s\left(\frac{1}{RC}+\frac{r}{L}\right)+\frac{1}{LC}} \quad (3)$$

where, V_{in} is the input DC voltage, L and C are output filter inductor and capacitor and r is the series leakage resistance for the filter capacitor. The input control signal to the buck converter is the duty cycle for the Pulse Width Modulation (PWM) which varies 0 through 1, and the output is the voltage across the heating element resistance.

The PWM block allows the controller to operate in CCM or DCM mode. In practice, an IC-PWM chip needs to be chosen, and associated gain K_{fb} needs to be determined. In our design, a unity K_{fb} was chosen for the PI controller and bang-bang controller, and a $K_{fb} = 10$ was used for the Phase Boost controller.

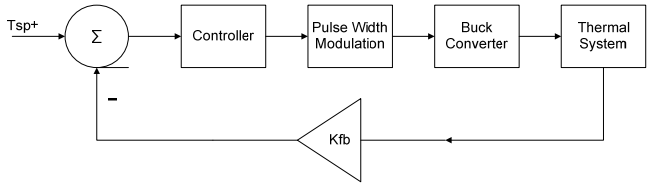

Figure 2 – Controller Block Diagram

A. Previosly Considered Control Strategies

1) Bang-Bang

In bang-bang or on/off control the electric heater is turned on to maximum power until a set-point is reached with an acceptable overshoot. Once the set-point is achieved, the heater turns completely off until the room temperature cools below an error threshold and then turns the heater back on.

In PSpice, this was simulated using a Schmitt Trigger circuit as seen in Figure 3. The R22 and R23 values were chosen to give a +/- threshold of 1° Celsius. The set-point is centered between the upper and lower threshold, and can be adjusted by changing V34 if desired.

2) Switching Strategies

Switching strategies are a type of direct control method for customer appliances. For these strategies, appliances have a modified circuit with switches that can be turned on or off at preferable times by a centralized controller. Since the appliances are aggregated they can provide ancillary services for utilities. A smart grid with two-way communication is needed for these systems [5].

3) Model Predictive Control (MPC)

MCP can use a wide number of inputs such as electricity cost, previous appliance history and in some cases weather information [12].

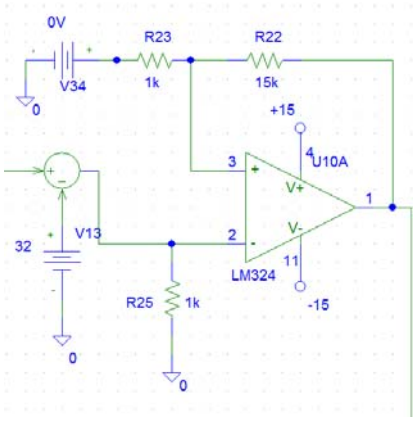

Figure 3– Bang-Bang Controller with Schmitt Trigger Stage

B. Linear Control Strategies for Space Heaters

The PWM stage determines when the buck converter is in the active or cutoff operation mode. For this project, an ideal transformer was used to represent a MOSFET, and a limit function was used for the PWM stage. Also, K_{fb} in Figure 4 is the gain for the feedback loop before the limit function and should be chosen to give a maximum duty cycle of 100%. A review of voltage control systems can be found in [11].

1) Phase Boost Controllers

The transfer function chosen for the controller can be seen in equation (4). The objectives when designing the controller were to maximize cross-over frequency f_c for fast response, a 60° phase margin for smooth settling, and a phase angle above $-180°$. Matlab was used in conjunction with the transfer function of the complete system to choose a cutoff frequency that gives 60° phase margin. The cutoff frequency is the point where the magnitude and phase of each transfer function are determined.

Since it is desirable to have a zero or minimal steady state error, the controller should have a pole at the origin which means the introduction of a $-90°$ phase angle in the open loop transfer function. The open loop transfer function phase for the system at f_c is $\angle G_{OL}(s) = -120°$ for 60° phase margin. A phase boost is calculated using (5) to achieve this phase margin. The controller parameter values k_c, ω_z and ω_p can then be calculated based on the design steps in reference [11].

$$G_C(s) = \frac{k_c}{s}\frac{\left(1+\frac{s}{\omega_z}\right)}{\left(1+\frac{s}{\omega_p}\right)} \quad (4)$$

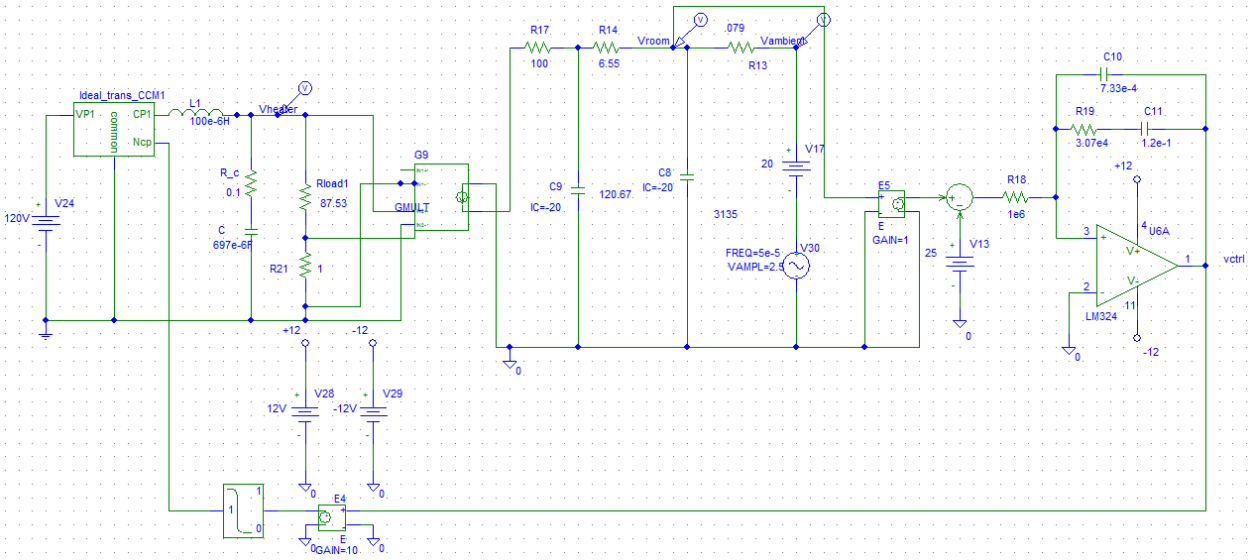

Figure 4 – Load Leveling System Schematic with Phase Boost Controller

$$\phi_{boost} = \angle G_{OL}(s) - \angle G_T(s) - \angle G_{PS}(s) + 90° \quad (5)$$

A circuit schematic of the phase boost controller implementation along with thermal system and power stage can be seen in Figure 4.

2) Proportional Integral Controller

A Proportional Integral (PI) controller was also tested with the thermal system. PI controllers allow steady-state error to approach zero, and fast convergence can be achieved when controller parameters are properly chosen. Also, PI controllers can be utilized for nonlinear system control applications.

For this simulation a P-term: K_p = 1 and I-term: K_i = 0.005 were found for a satisfactory performance. The feedback gain K_{fb} term was set to 1 for the PI controller. A PSpice circuit implementation for a PID controller can be seen in Figure 5. The P-term is found from the ratio of $\frac{R31}{R29}$, while the I-term is found from the ratio of $\frac{C16}{R29}$. The D-term of a PID controller is found using C17 but is voided in this simulation with an open switch. The transfer function for the PID controller can be seen in Equation (6).

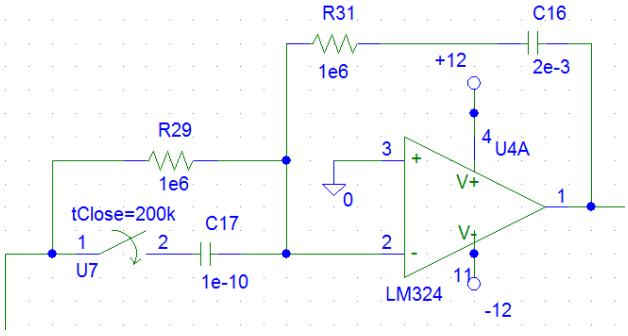

Figure 5 - PI controller Schematic

$$G_C(s) = \frac{K_d s^2 + K_p s + K_i}{s} \quad (6)$$

IV. Results

The controllers were simulated with thermal system parameters obtained from the system identification tests. Linear control schemes were compared to a bang-bang controller. The rise time, steady state errors, steady state ramp rates in power drawn for each test were also found.

For each simulation, two linear controllers were plotted on the same graph, and the bang-bang controller was plotted separately. The V_{heater} (V_h) was plotted for each controller where V_h corresponds to the Voltage on the load (heater) resistor. V_h is plotted with thicker lines than the V_{room}, and V_{room} has the same color for the corresponding controller. $V_{ambient}$ is also plotted in black for each controller. Each model was tested with the set point used for the identification of that model. A sinusoidal ambient temperature was also used with $\pm 2.5°C$ range and $Period = 20000$ seconds. Since the temperature range was close to the identification point, it was assumed that the thermal model was still valid.

The controllers all converged to the correct V_{room} set-point. However, it is clear that linear controller peak voltage demand at steady state is significantly lower than bang-bang controller.

A. Simulations with Constant Ambient Temperature

The peak power demand reduction can be seen by comparing the maximum steady state voltage between linear and bang-bang controllers. In all tests the steady state operating voltage is the same for both linear controllers. In Model 2, the bang-bang controller uses a V_{heater} of 120V at steady state while the linear controllers converge to 80V as seen in Figures 8 and 9. The peak demand reduction is approximately 33% for this test. With a lower operating point,

the Voltage reduction is greater, and the reduction is much lower for Model 1 for this reason. Since this voltage was applied to a resistor, the current will also be smaller at the same rate as voltage. Using $P = V^2 / R$ formula, this translates into 55.6 % peak power demand reduction.

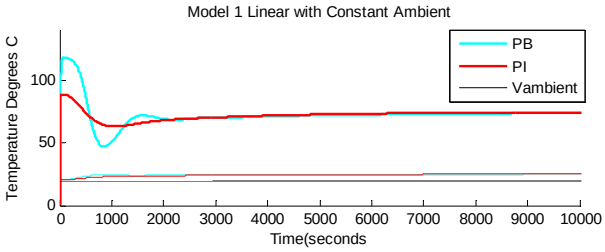

Figure 6–Linear controllers at 25^0 Set point and constant 20^0 ambient temperature (PB: Phase Boost, PI: PI Controller)

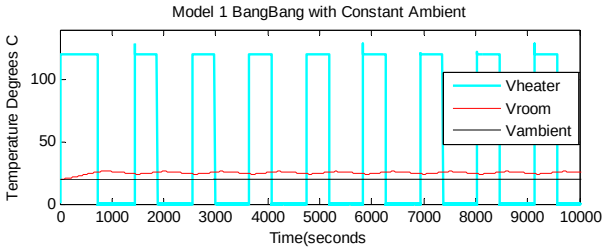

Figure 7 –BangBang controller at 25^0 Set point and constant 20^0 ambient temperature

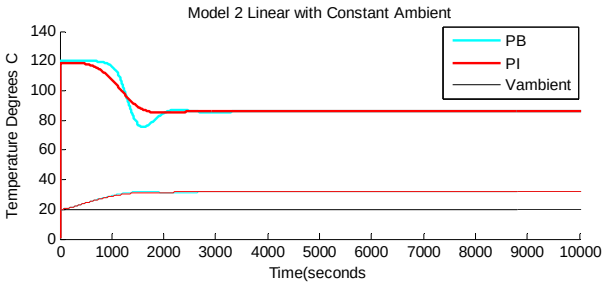

Figure 8 –Linear controllers at 30^0 Set point and constant 20^0 ambient temperature (PB: Phase Boost, PI: PI Controller)

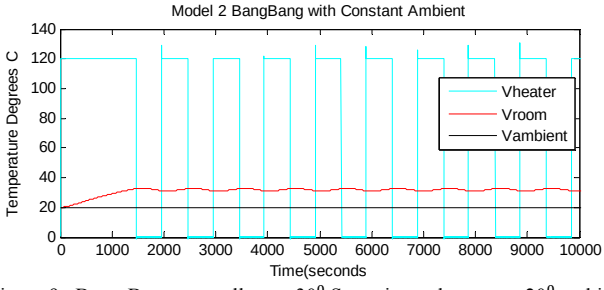

Figure 9 –Bang-Bang controllers at 30^0 Set point and constant 20^0 ambient temperature

B. Simulations with 17.5°- 22.5° Variable Ambient Temperature

The next test had a variable ambient temperature. The linear controller adjusts the operating voltage to match the ambient temperature based on the changes in the feedback control signal. The bang-bang controller changes the duty cycle in order to accomplish this, but always demands the maximum voltage which is 120 Volts. Plots of simulations can be seen in Figures 10-13.

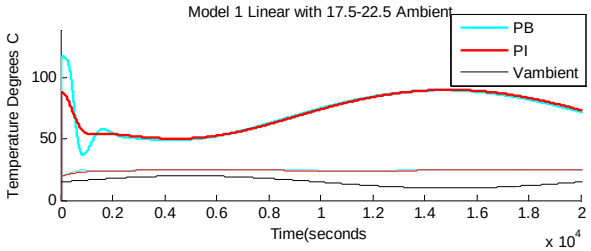

Figure 10 – Linear controllers at 25^0 Set point with 17.5-22.5^0 ambient temperature (PB: Phase Boost, PI: PI Controller)

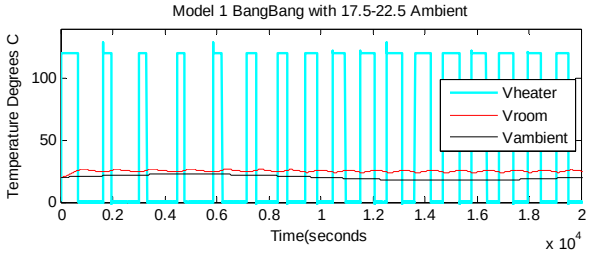

Figure 11 – Bang-Bang 25^0 Set point with 17.5-22.5^0 Ambient BangBang Controller

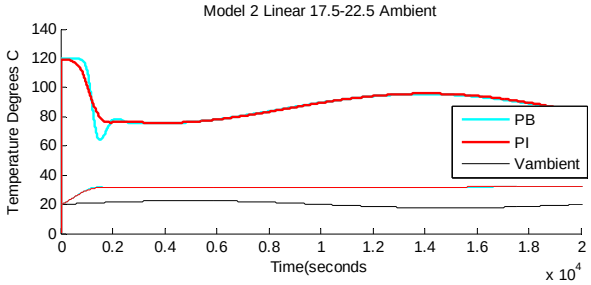

Figure 12 – Linear controllers at 32^0 Set point with 17.5-22.5^0 Ambient Temperature (PB: Phase Boost, PI: PI Controller)

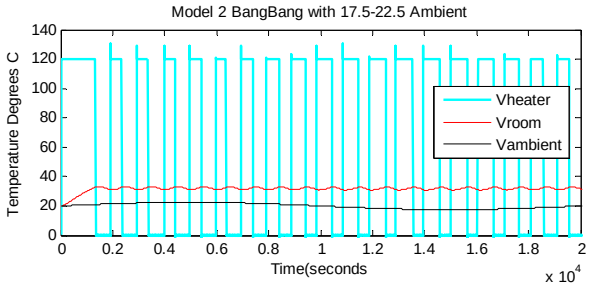

Figure 13 – Bang-Bang Controller at 32^0 Set point with 17.5-22.5^0 Ambient temperature

The peak demand reduction is also evident with the linear controllers as can be seen Figures 10 and 12.

C. Controller Performance Comparisons

Resulting performance was evaluated for both Model 1 and 2 as seen in Tables 3 and 4. Rise time was calculated as the time it takes V_{room} to reach 95% of the set point temperature. The maximum and minimum errors for steady state operations were also calculated. All controllers performed well and had

negligible errors at steady state. The PI controller converged much slower for the Model 1, but stayed within a close tolerance once it converged. The phase boost controller had the least error margins and similar rise times to the bang-bang controller. The bang-bang controller always had the largest error because of the turn on and turns off temperatures from the Schmitt trigger. Decreasing the temperature range of a bang-bang controller apparently requires more switching.

TABLE 3 – Thermal Model 1 Rise Time, Max and Min Errors

	Model 1				
Controller	***(°C) Set point***	***(°C) Ambient***	***(Seconds) Rise Time***	***(°C) Max error***	***(°C) Min error***
Phase Boost	25	20	596	0.04	0.04
PI	25	20	2312	0.05	0.05
BangBang	25	20	507	1.04	0.91
Phase Boost	25	17.5-22.5	556	0.36	0.44
PI	25	17.5-22.5	1368	0.52	0.62
BangBang	25	17.5-22.5	485	1.40	1.11

TABLE 4 – Thermal Model 2 Rise Time, Max and Min Errors

	Model 2				
Controller	***(°C) Set point***	***(°C) Ambient***	***(Seconds) Rise Time***	***(°C) Max error***	***(°C) Min error***
Phase Boost	32	20	1159	0.04	0.04
PI	32	20	1280	0.05	0.05
BangBang	32	20	1147	0.93	1.04
Phase Boost	32	17.5-22.5	1074	0.23	0.32
PI	32	17.5-22.5	1169	0.32	0.41
BangBang	32	17.5-22.5	1062	1.06	1.18

D. Maximum and Minimum Demand Ramp Rates

The power demand ramp rates or voltage slopes were also measured for the controllers in *Volts/Hour* for Model 1 as seen in Table 5. The results were also pretty similar with Model 2. These voltage slopes were calculated for the steady state operation. The ramp rates were smallest with the phase boost controller. On the other hand, the ramp rate was always large for bang-bang controllers, even when the outside temperature is constant. The slopes were close to zero for linear controllers at steady state with a constant ambient temperature testing.

TABLE 5 – Thermal Model 1 based Max and Min Slope

	Model 1			
Controller	***(°C) Set point***	***(°C) Ambient***	***(Volt / Hour) Max Slope***	***(Volt / Hour) Min Slope***
Phase Boost	25	17.5-22.5	0.44	-0.49
PI	25	17.5-22.5	0.65	-0.74
BangBang	25	17.5-22.5	2721.50	-2721.50

V. CONCLUSION

Space heating appliance control methodology discussed in this paper can lead the way to more control methodologies that are not often investigated for appliances such as air conditioners, refrigerators, EWH's, and ovens/hotplates.

It was shown in this paper that the linear control methods discussed can effectively reduce peak demand and demand ramp rates which are desirable features for utilities and smart grid settings.

It was also shown that proper system identification is a key component of designing a linear controller. The thermal system model provided the specifics of design sequence for the phase boost controller which clearly outperformed any other controller tested.

In order to verify whether the controllers would work with the actual enclosure in similar manner requires the next step of experimental testing.

ACKNOWLEDGMENT

The authors wish to thank the Center for Rapid Product Realization at Western Carolina University, Prof. Gardner and Prof. Zhang for the project support, and Prof. Adams and Prof. Yanik for helpful suggestions.

REFERENCES

[1] P. Waide, J. Amann and A. Hinge, "Energy efficiency in the north american existing building stock," OECD/IEA, France, 2007.

[2] T. Broeer, J. Fuller, F. Tuffner, D. Chassin and N. Djilali, "Modeling framework and validation of a smart grid and demand response system for wind power integration," Appl. Energy, vol. 113, pp. 199-207, 1, 2014.

[3] N. Lu, M. R. Weimar, Y. V. Makarov, J. Ma, and V. V. Viswanathan,The wide-area energy storage and management system—Battery storage evaluation, PNNL-18679, Pacific Northwest National Laboratory. Richland, WA, 2009.

[4] D. S. Callaway, "Can smaller loads be profitably engaged in power system services?" in *Power and Energy Society General Meeting, 2011 IEEE,* 2011, pp. 1-3.

[5] J. Kondoh, Ning Lu and D. J. Hammerstrom, "An Evaluation of the Water Heater Load Potential for Providing Regulation Service," *Power Systems, IEEE Transactions* on, vol. 26, pp. 1309-1316, 2011.

[6] M. H. Nehrir, Runmin Jia, D. A. Pierre and D. J. Hammerstrom, "Power management of aggregate electric water heater loads by voltage control," in Power Engineering Society General Meeting, 2007. IEEE, 2007, pp. 1-6.

[7] H. Dean Venable, "The K-Factor: A New Mathematical Tool for Stability Analysis and Synthesis," Proceedings of Powercon 10, http://www.venable.biz.

[8] Ion Hazyuk, Christian Ghiaus, David Penhouet, "Optimal temperature control of intermittently heated buildings using Model Predictive Control Part I Building modeling," Building and Environment 51 (2012) pp 379-387, Elsevier.

[9] Matlab 2012a System Identification Toolbox.

[10] Pspice version 9.1

[11] N. Mohan, Power Electronics A First Course. MA: John Wiley & Sons, Inc., 2012.

[12] S. Prívara, J. Široký, L. Ferkl and J. Cigler, "Model predictive control of a building heating system: The first experience," Energy Build., vol. 43, pp. 564-572, 0, 2011.